Review Article

Magnetic resonance imaging of paraurethral and paravaginal lesion: relevant diagnoses, key findings and surgical correlation

Andrés Labra[1], Rolando Cocio[1], Álvaro Saavedra[2], Giancarlo Schiappacasse[1], Fernanda Blaskovic[3]^

[1]Department of Radiology, Clínica Alemana de Santiago, Santiago, Chile; [2]Department of Urology, Clínica Alemana de Santiago, Santiago, Chile; [3]Department of Radiology, Clínica Alemana de Santiago-Universidad del Desarrollo, Santiago, Chile

Contributions: (I) Conception and design: A Labra, F Blaskovic, R Cocio; (II) Administrative support: G Schiappacasse; (III) Provision of study materials or patients: A Labra, Á Saavedra; (IV) Collection and assembly of data: A Labra, R Cocio, F Blaskovic; (V) Data analysis and interpretation: All authors; (VI) Manuscript writing: All authors; (VII) Final approval of manuscript: All authors.

Correspondence to: Fernanda Blaskovic, MD. Department of Radiology, Clínica Alemana de Santiago-Universidad del Desarrollo, Av. Manquehue 5951, Vitacura, Santiago, Chile. Email: fblaskovic@alemana.cl.

Abstract: Paraurethral and paravaginal lesions are uncommon entities that often present diagnostic challenges due to their anatomical complexity, varied etiologies, and overlapping clinical presentations. Accurate identification and characterization of these lesions are essential for appropriate management and surgical planning. A structured diagnostic approach, based on clinical history, lesion location, and imaging features, is critical to avoid misdiagnosis and unnecessary interventions. Magnetic resonance imaging (MRI) has emerged as the modality of choice due to its excellent soft-tissue contrast, multiplanar capabilities, and non-invasive nature, offering superior delineation of lesion extent and relationship with adjacent pelvic structures. This pictorial review seeks to support radiologists and clinicians by offering a comprehensive yet practical guide to the imaging evaluation of paraurethral and paravaginal lesions. Through high-resolution MRI images and original anatomical illustrations, we aim to reduce the gap between imaging interpretation and clinical decision-making. We summarize the primary MRI indications for evaluating female urethral pathology, provide an overview of common and rare differential diagnoses, and highlight relevant MRI protocol considerations. Additionally, we include correlations with surgical findings when available, to enhance clinical applicability. Rather than providing an exhaustive catalog of entities, our focus is to promote standardized imaging assessment and highlight key anatomical and diagnostic considerations that may facilitate a more confident and informed multidisciplinary approach to these often-overlooked pelvic pathologies.

Keywords: Paraurethral lesions; paravaginal lesions; magnetic resonance imaging (MRI); differential diagnosis; pelvic imaging

Submitted Dec 18, 2024. Accepted for publication Apr 01, 2025. Published online May 27, 2025.
doi: 10.21037/tau-2024-726
View this article at: https://dx.doi.org/10.21037/tau-2024-726

^ ORCID: 0009-0008-4101-0009.

Introduction

Background

Paraurethral and paravaginal lesions in women are a rare diagnosis, in most cases they present nonspecific symptoms. Soft tissue ultrasound of the vaginal introitus and transvaginal ultrasound are being of great help in the characterization of lesions in the office as a complement to the physical examination, although it lacks contrast resolution to detect the origin of small lesions and their relationship with adjacent structures (1). Magnetic resonance imaging (MRI) is the method of choice for surgical planning, as well as for lesions that require a better diagnostic characterization (2,3). The following article aims to make a pictorial review of the main characteristics of these lesions, emphasizing the characteristics by MRI, distinguishing the most frequent differential diagnoses and systematizing their analysis, mainly based on their distribution.

Rationale and knowledge gap

Paraurethral and paravaginal lesions in women may manifest with diverse and nonspecific genitourinary symptoms or as an incidental finding in an asymptomatic patient (2-4). The most frequent symptoms are mass, dysuria, pelvic pain, urinary frequency, dyspareunia, pus per urethra, stress incontinence, and recurrent urinary tract infections. It is important to identify each of the etiologies to avoid unnecessary interventions. In cases of diagnostic doubt, images provide optimal sensitivity and specificity for most entities (5).

Objective

This pictorial review provides a systematic and comprehensive overview of paraurethral and paravaginal lesions in women, integrating current literature and local clinical experience. As a pictorial, it emphasizes imaging findings, particularly MRI features, alongside key anatomical landmarks and surgical correlation. The goal is to support radiologists and clinicians in improving diagnostic accuracy and optimizing clinical management of these lesions, which, although variable in prevalence, are all clinically significant and may present with complex features and potential complications.

Diagnostic and imaging-based approach to paraurethral and paravaginal lesions: anatomical overview and key differentials

MRI has been consistently reported to have a higher sensitivity and predictive value than voiding cystourethrography or double-balloon positive pressure retrograde urethrography for detecting female urethral and periurethral disorders (6-8). Ultrasonography, especially in its transvaginal, transperineal and transurethral modalities, is more accessible than MRI and has a high performance in cystic lesions, in addition to the absence of radiation and the ability to obtain images in real time; however, it has lower sensitivity and specificity (80% and 65% respectively) to visualize deep or small structures as well as to characterize the relationship of the lesion with neighboring structures. Due to the good contrast resolution and anatomical correlate of MRI, it allows to differentiate the origin and content of the lesion with a sensitivity of 85–95% and a specificity between 90–97% (1,9,10). On the other hand, it plays a fundamental role in surgical planning if necessary (1,9-11). One of the reasons that justifies the diagnostic effort of this type of lesions is the possible associated complications, for example, the superinfection of a Bartholin cyst or malignancy as in the urethral diverticulum that merit specific management (3-5).

Based on a focused literature review, four structured tables were developed to provide an imaging-based framework for evaluating paraurethral and paravaginal lesions. *Table 1* summarizes key MRI indications (1,4), while *Table 2* outlines main differential diagnoses by frequency and imaging features (2,10,11), including enhancement patterns and urethral communication (12). *Table 3* presents a standardized MRI protocol, and *Table 4* integrates anatomical and radiological findings to support consistent reporting and surgical planning. These tables complement the text and the original illustrations created by the authors, helping to better understand imaging findings and the diagnostic process of these lesions. *Figures 1,2* provide a didactic overview of paraurethral and paravaginal lesions, highlighting key anatomical landmarks. *Figure 3* summarizes their spatial distribution and was designed as a quick-reference visual tool to facilitate lesion localization through anatomical landmarks and thereby narrow the differential diagnosis during imaging evaluation, particularly in relation to the

Table 1 Summary of the main indications for MRI study of the female urethra

Type of abnormality	General indications
Structural type	Suspected urethral diverticulum, suspected periurethral mass, urethral neoplasia, and known or suspected fistula
According to symptoms	Persistent urinary symptoms despite conventional treatment, recurrent urinary tract infections
Functional type	Suspected prolapse and urinary incontinence
Related to the patient	Pregnancy, young patients, and patients who do not wish to undergo studies with radiation

Summary of primary MRI indications for evaluating paraurethral and paravaginal pathologies (1,3). Conditions were selected based on prevalence and clinical relevance, including both common and diagnostically complex entities to ensure practical value for radiologists and clinicians. MRI, magnetic resonance imaging.

Table 2 Clinical features and frequency of paraurethral and paravaginal lesions

Injury	Location	Symptoms/physical exam	Estimated frequency (%)
Skene's gland cysts	Inferior and lateral to the meatus	Painful, visible ductal orifice at the urethral meatus	10–30
Urethral caruncle	Inferior to the meatus	Asymptomatic or dysuria/pain with atrophic or ischemic mucosal changes	3–15
Urethral diverticulum	Anterior vaginal wall, periurethral, midline	Urinary tract infections, dysuria, dyspareunia, post-micturition dribbling, cystic mass	1–6
Urethral mucosal prolapse	Circumferential mucosal prolapse with central meatus	Pain and dysuria, atrophic or ischemic mucosal changes	1–4
Urethral tumors (benign/ malignant)	Urethral or vaginal wall or hematuria	Solid mass; may be painful, may be visible on cystoscopy	<1

Main differential diagnoses of paraurethral and paravaginal lesions, listed by frequency and clinical relevance, including Skene's gland cysts, caruncles, urethral diverticula, Gartner's duct cysts, Bartholin's gland cysts, epidermal inclusion cysts, and neoplastic lesions (2,10,12). Differentiating features include signal intensity, contrast enhancement patterns (IVC), communication with the urethra, axial and longitudinal position, and post-void morphology (4,5,13). IVC, intravenous contrast.

Table 3 Summary of the female urethral MRI protocol

Sequences	Flat	Technical characteristics
T2WI FSE	Sagittal	3 mm/0.3 mm, FOV 16 cm
T2WI FSE	Coronal	Axis parallel to urethra 2.5 mm/0.2 mm, FOV 16 cm
T2WI FSE	Axial	Axis perpendicular to urethra 2.5 mm/0.2 mm, FOV 16 cm
T2WI FSE fat sat	Axial	Axis perpendicular to urethra 3 mm/0.3 mm, FOV 16 cm
T1WI FSE	Axial	Axis perpendicular to urethra 3 mm/0.3 mm, FOV 18 cm
Diffusion	Axial	B0 (1 NEX), B50 (2 NEX) and B800 (10 NEX), axis perpendicular to the urethra 4 mm/0.4 mm, FOV 18 cm
ADC	Axial	–
T1 fat sat without and with CIV	Axial	Perpendicular axis to urethra 1 mm, FOV 22–24 cm
T1 fat sat with CIV	Coronal	Axis parallel to urethra 1 mm, FOV 22–24 cm
Subtraction	Axial	–

Overview of the main parameters of the MRI protocol used for female urethral imaging. Designed to promote protocol standardization and ensure optimal evaluation of the paraurethral region. ADC, apparent diffusion coefficient; CIV, intravenous contrast; fat sat, fat saturation; FOV, field of view; FSE, fast spin echo; MRI, magnetic resonance imaging; NEX, number of excitations; T1WI, T1-weighted imaging; T2WI, T2-weighted imaging.

Table 4 Summary of the main clinical-radiological considerations of urethral, paraurethral, and paravaginal injuries

Type of injury	Anatomical considerations	MRI
Gartner cyst	Cystic lesion arising from the anterolateral upper vaginal wall	The report should include size, location, anatomic relationships, and evidence of complication
Skene's gland cyst	Paraurethral cyst, at the level of the posterolateral aspect of the distal urethra	The report should include size, location, relationship to the meatus, evidence of superinfection or elements of malignancy
Urethral diverticulum	Lesions acquired at the level of the ventrolateral aspect of the middle and proximal third of the urethra. Generally incidental	The report should include size, location, number and evidence of complication. Complement with pre- and post-voiding sequences
Bartholin's gland cyst	Cystic lesion in the posterolateral vaginal introitus	The report should include size, location, type of enhancement, signs suggesting superinfection or malignancy
Vulvar epidermal inclusion cyst	Skin nodules generally located on the labia majora	The report must include size, location, and relationship to the CIV

Integration of anatomical and imaging features by lesion type. Offer a structured guide for reporting that supports consistent interpretation and highlights findings relevant for diagnosis, staging, and surgical planning. CIV, intravenous contrast; MRI, magnetic resonance imaging.

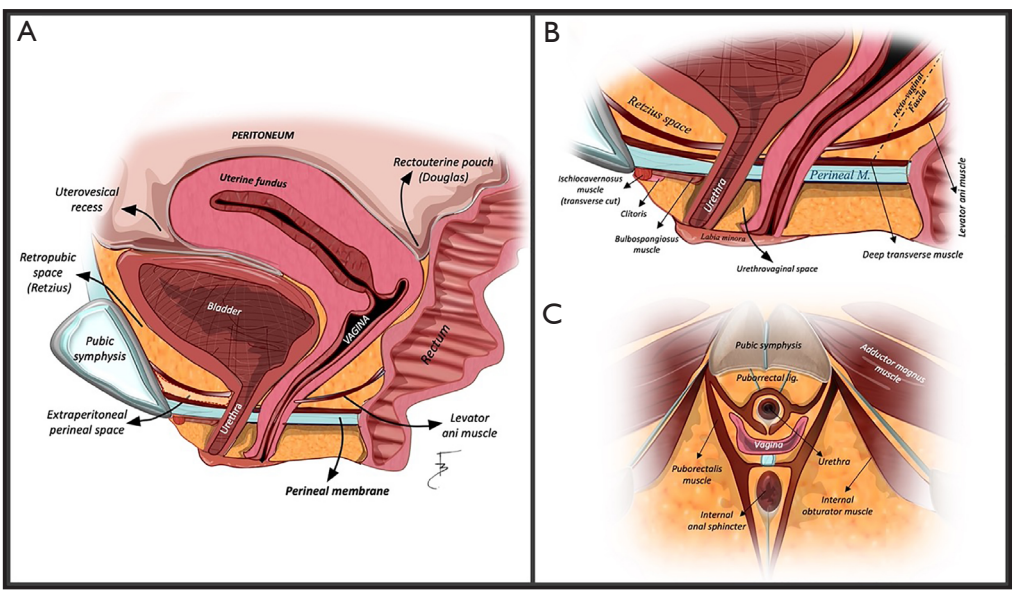

Figure 1 Author-generated anatomical illustration showing sagittal (A,B) and axial (C) views of the pelvis. The most relevant anatomical structures evaluated on MRI for the diagnosis of paraurethral and paravaginal lesions are labeled (illustration created by the authors). MRI, magnetic resonance imaging.

perineal membrane.

For didactic purposes, they were subdivided into three groups according to their etiology: cystic, miscellaneous or neoplastic.

Cystic paraurethral-paravaginal lesions

Urethral diverticulum

This is a lesion that is most frequently acquired and could be derived from the obstruction of the paraurethral

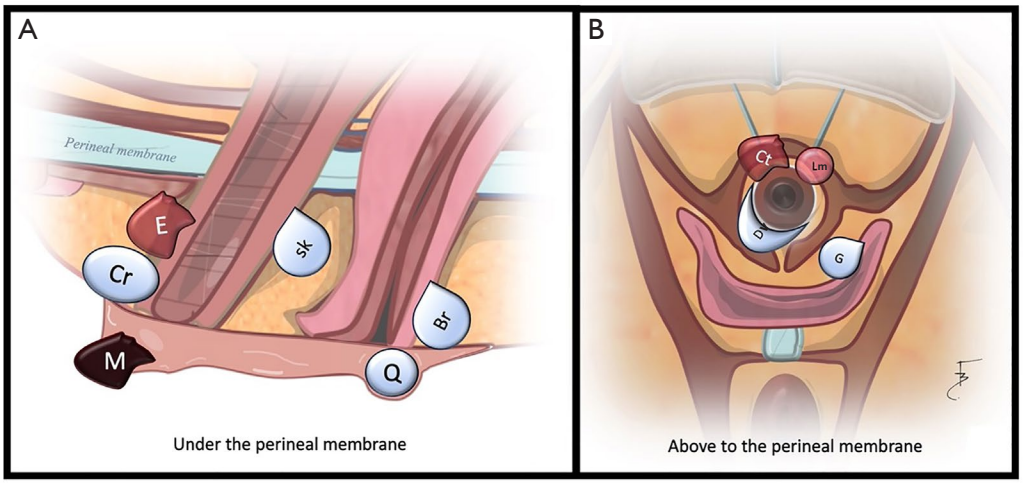

Figure 2 Author-generated anatomical diagrams in sagittal (A) and axial (B) views, showing the paraurethral and paravaginal lesions included in this review. The illustrations highlight their anatomical location relative to the PM and nearby pelvic structures. Urethra: distal to the PM: Sk, Cr, and E; proximal to the PM: Dv, Lm, and Ct. Vagina: distal to the PM: Br; labia minora: Q and M; proximal to the PM: G. Br, Bartholin's gland cyst; Cr, caruncle; Ct, transitional cell carcinoma; Dv, urethral diverticula; E, squamous cell carcinoma; G, Gartner's duct cyst; Lm, leiomyoma; M, melanoma; PM, perineal membrane; Q, epidermal inclusion cyst; Sk, Skene's gland cyst.

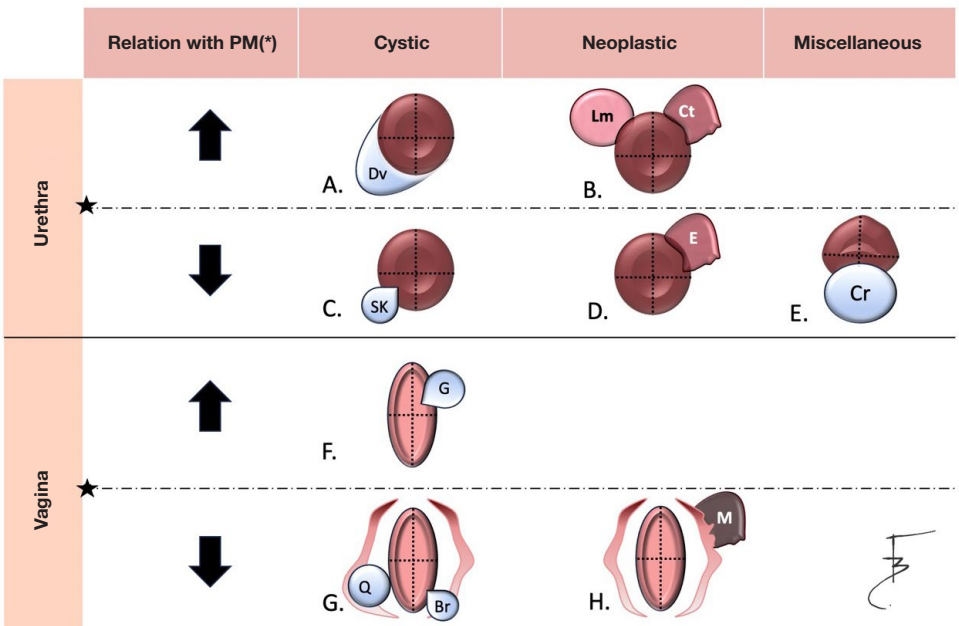

Figure 3 Author-generated schematic diagram summarizing the anatomical distribution of paraurethral and paravaginal lesions (13). Designed as a quick-reference visual tool to support differential diagnosis through anatomical localization—particularly in relation to the perineal membrane (PM, star). Spatial relationships of cystic, neoplastic, and miscellaneous lesions affecting the urethra and vaginal wall are illustrated. Urethra: proximal to the PM: (A) Dv; (D) E; distal to the PM: (B) Ct and Lm; (C) Sk; (E) Cr. Vagina: proximal to the PM: (H) M; distal to the PM: (F) G; (G) Q and Br. Br, Bartholin's gland cyst; Cr, caruncle; Ct, transitional cell carcinoma; Dv, urethral diverticula; E, squamous cell carcinoma; G, Gartner's duct cyst; Lm, leiomyoma; M, melanoma; PM, perineal membrane; Q, epidermal inclusion cyst; Sk, Skene's gland cyst.

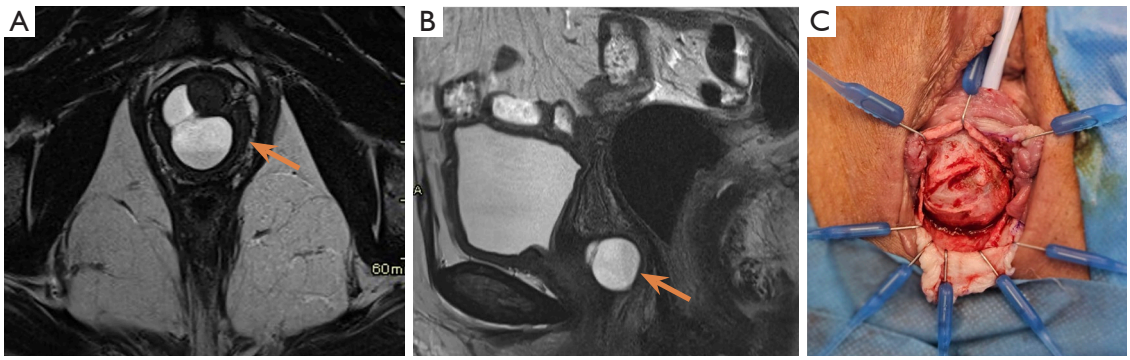

Figure 4 Pelvic MRI with VSD showing a saddle-shaped urethral diverticulum (orange arrows) in the right posterolateral aspect of the mid-urethra. The lesion appears hyperintense on T2-weighted images (A,B) and hypointense on fat-saturated T1 images. Post-contrast VSD images show peripheral enhancement. No signs of complication are seen. Intraoperative images show the diverticulum exposed through an inverted U-shaped anterior vaginal wall incision and horizontal dissection of the periurethral fascia (C). MRI, magnetic resonance imaging; VSD, vaginal saline distension.

glands, with subsequent formation of a collection that communicates with the urethral lumen, which constitutes the diverticulum itself. Other less frequent causes are postpartum urethral injury, or Müllerian duct cysts (4,5,14). There are series that indicate that up to 6% of women will present this condition at some point in their life, with an average age between 30 and 50 years. Most urethral diverticula are asymptomatic and constitute incidental findings in imaging studies. If symptoms exist, they may include mass, dysuria, pelvic pain (12,15,16), among others. They may rarely be complicated by stone formation (10%) or malignant transformation in up to 4–10% (adenocarcinoma or Urothelial carcinoma) representing only 5% of all female urethral cancers (6,12,17-19). In certain cases, antibiotic therapy is necessary to treat superinfection prior to definitive surgical intervention, such as diverticulectomy. Recurrence factors have been described after surgical treatment, including large size (greater than 4 cm), incomplete resection of the diverticular neck, proximal location and "saddle" morphology (2,3,5).

On MRI, urethral diverticula (*Figure 4*) appear as uni- or multilocular T2 hyperintense cystic lesions, typically >2 cm, located posterolaterally in the mid or proximal urethra. Post-void enlargement and identification of the diverticular neck are key findings. Signs of complications include wall thickening, restricted diffusion, low apparent diffusion coefficient (ADC) signal, and peripheral enhancement with contrast (1,3,5,14).

A complicated urethral diverticulum on contrast-enhanced CT typically appears as a complex periurethral cystic lesion (*Figure 5*) with internal septations, heterogeneous content, and mild wall enhancement, which may indent adjacent structures such as the bladder trigone. MRI further characterizes the lesion, confirming multilocular morphology, thickened enhancing walls, and diffusion restriction, allowing precise evaluation of extent, internal architecture, and signs of superinfection or inflammation (20).

Skene's gland cyst

The Skene's gland corresponds to an analogue of the prostate gland, which is located along the distal urethra in a posterolateral position (3 to 9 according to the time signal), distal to the perineal membrane, fulfilling the function of providing urethral lubrication (6,8,17). In total, there are no more than 4 glands. Cysts arise due to obstruction of the ostium and occur more frequently between 30 and 40 years of age. Their content may be liquid, high in protein, bloody or purulent, in case of complications, with Neisseria gonorrhoeae being the most frequent microorganism isolated in case of superinfection (8). Generally, they are asymptomatic and only cause discomfort depending on the size or eventual complication (3,4). The treatment is adjusted according to the type of complication, without the need for specific management if they are asymptomatic.

On MRI, Skene gland cysts (*Figures 6,7*) appear as small (<2 cm), rounded, oval, or teardrop-shaped lesions located

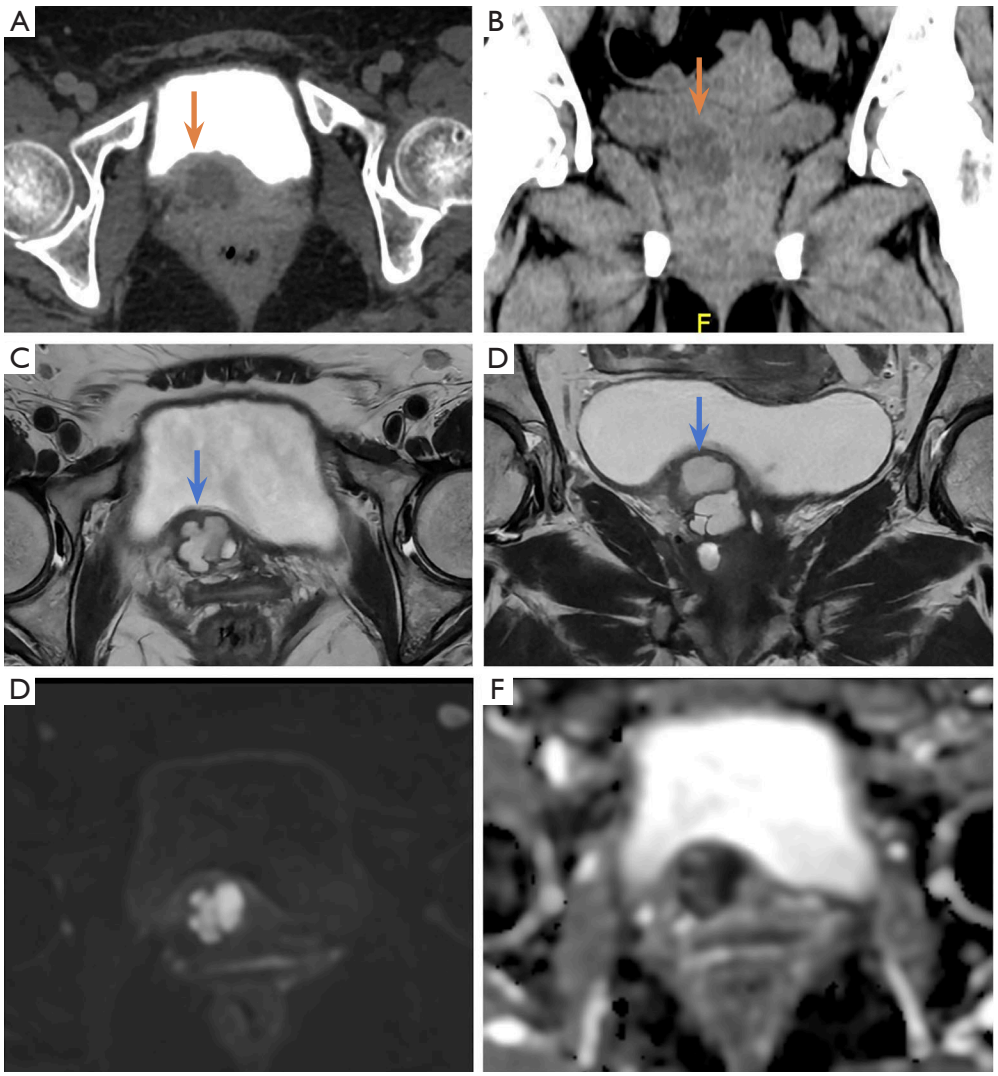

Figure 5 Uro-CT and MRI correlation in a complicated urethral diverticulum. (A,B) Uro-CT: right-sided complex cystic lesion (orange arrows) with septations, heterogeneous content, and mild wall enhancement, displacing the bladder trigone. (C-F) MRI: a multilocular paraurethral cystic lesion (blue arrows) with thick enhancing septa and heterogeneous diffusion restriction (E,F). CT, computed tomography; MRI, magnetic resonance imaging.

posterolaterally in the distal urethra, below the perineal membrane and at the lower margin of the pubic bone. Uncomplicated cysts are homogeneously hypointense on T1 and hyperintense on T2 sequences (2,3,11). When complicated by superinfection or hemorrhage, they may exhibit T1 hyperintensity and T2 hypointensity due to their internal content. Malignancy of the Skene gland is rare. Twenty-two cases have been reported to date (3,17,21), and should be suspected in the case of thickening and nodular appearance intravenous contrast (IVC) enhancement, associated with an increase in serum prostate antigen in these cases (6). Recognizing and further evaluating paravaginal lesions detected on CT is crucial. On non-contrast CT, Skene gland cysts may appear as well-defined, low-attenuation cystic lesions in the urethrovaginal region, occasionally mimicking Bartholin's cysts. In this case, the lesion was identified on the final acquisition slices and initially misinterpreted, with subsequent MRI confirming

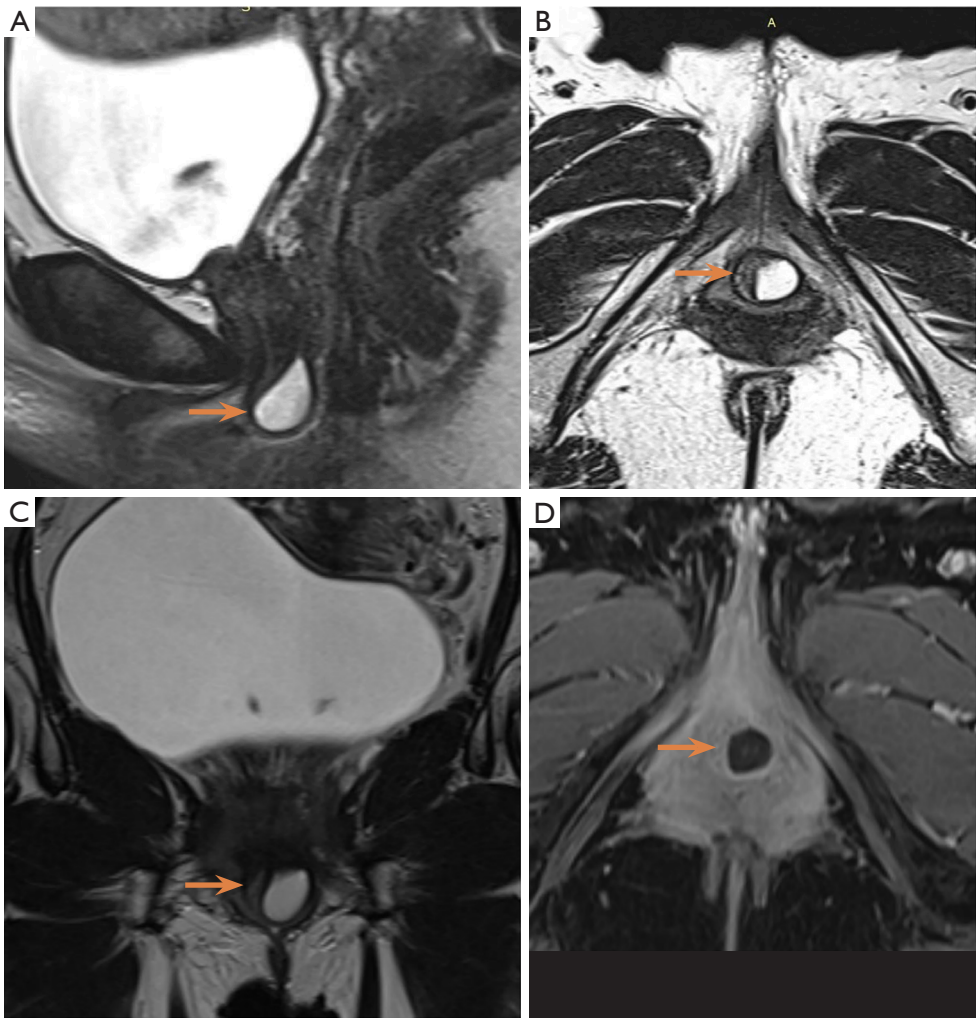

Figure 6 Pelvic MRI with VSD showing a left-sided, posterolateral, teardrop-shaped Skene's gland cyst (orange arrows) in the distal third of the urethra. The lesion appears hyperintense on T2-weighted images (A-C) and shows minimal peripheral enhancement on T1 fat-saturated post-contrast imaging (D). No signs of complication are present. MRI, magnetic resonance imaging; VSD, vaginal saline distension.

the diagnosis of a large Skene gland cyst (*Figure 8*).

Gartner's cyst [remnant of the mesonephric duct (Wolffian)]

It is one of the most frequent lesions, representing about 11% of all vaginal cysts (12,22). They are generally asymptomatic, but when symptoms are present, they include pelvic pain and dyspareunia (3,23,24). The age of presentation is between 30 and 50 years. It may be associated with other alterations of the genitourinary system such as renal dysplasia, renal agenesis, crossed renal ectopia and Müllerian anomalies, so it is recommended to perform complementary studies directed to rule out these entities (25,26). Most Gartner's cysts do not require specific treatment.

On MRI, Gartner's cysts (*Figure 9*) appear as solitary lesions in the upper third of the vagina, anterolateral to the vaginal wall and proximal to the perineal membrane. They show high signal on T2-weighted sequences, without diffusion restriction or contrast enhancement, and maintain a clear separation from the cervix and urethra. In rare cases, they may complicate with superinfection,

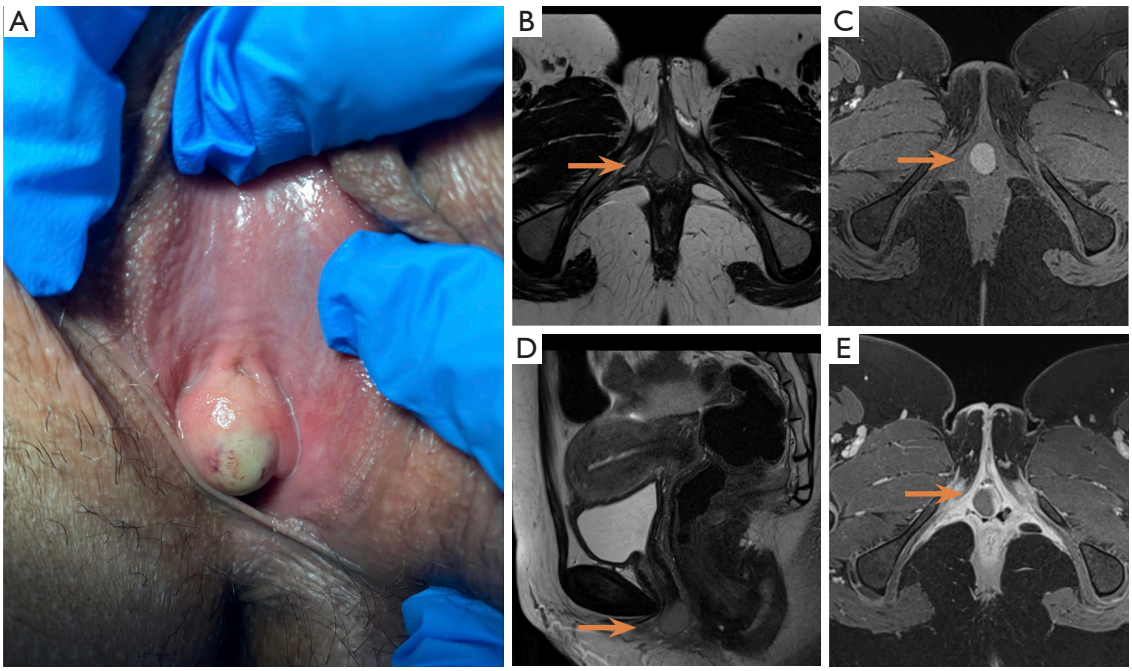

Figure 7 MRI and clinical correlation of a superinfected Skene's gland cyst. (A) Preoperative clinical photograph showing the lesion. (B,D) Axial and sagittal T2-weighted MRI showing the lesion as hypointense. (C) Axial fat-saturated T1-weighted image demonstrates hyperintensity of the lesion. (E) Post-contrast T1-weighted image shows wall enhancement, suggesting purulent or proteinaceous content. Orange arrows indicate the lesion in each panel. MRI, magnetic resonance imaging.

hemorrhage, or malignant transformation to clear cell adenocarcinoma (9,17,24).

Bartholin's gland cyst

Normal Bartholin's glands are located bilaterally at the posterior vaginal introitus at the base of the labia majora. Normal glands measure between 0.5 to 1 cm, with drainage ducts emptying between 4 and 8 o'clock according to the time signal along the introitus. Their function is to contribute to vulvovaginal lubrication (2-5,10). Cysts arise secondary to obstruction of the drainage tracts, and some causes of obstruction are history of vulvovaginal surgery, trauma, thick discharge, stones, and previous infections. The age of presentation ranges between 20 and 30 years, and it is estimated that 2% of women will develop a Bartholin's cyst or abscess. Cysts may be complicated by infection and rupture. Cultures are generally polymicrobial and include *Neisseria gonorrhoeae* and *Chlamydia trachomatis*. Clinically, they manifest as a focal posterior vulvar bulge, associated with inflammatory symptoms. Treatment will depend on whether it presents with superinfection or not (10).

On MRI, Bartholin's gland cysts (*Figure 10*) appear as T2 hyperintense cystic lesions without diffusion restriction or contrast enhancement. They are located below the perineal membrane, in the lateral aspect of the lower third of the vagina, projecting toward the vaginal introitus, with no anatomical connection to the urethra. Malignancy is rare and should be suspected in the presence of nodular-appearing enhancements and in patients older than 40 years (9).

Vulvar epidermal inclusion cyst

This is a skin lesion caused by the proliferation of squamous epithelium. It is the most common type of cystic lesions of the vulva in any age group. They can be caused by trauma, in these cases it is postulated that a bad folding of the skin planes is caused, producing the inclusion cyst (27). Most are asymptomatic and do not require intervention, however, in isolated cases they can be large, cause pain or become infected, indicating antibiotic therapy and subsequent excision. Recurrence reaches up to 50%, depending on the total or partial removal of the capsule (4,27). It should be considered within the differential diagnosis of paraurethral-paravaginal

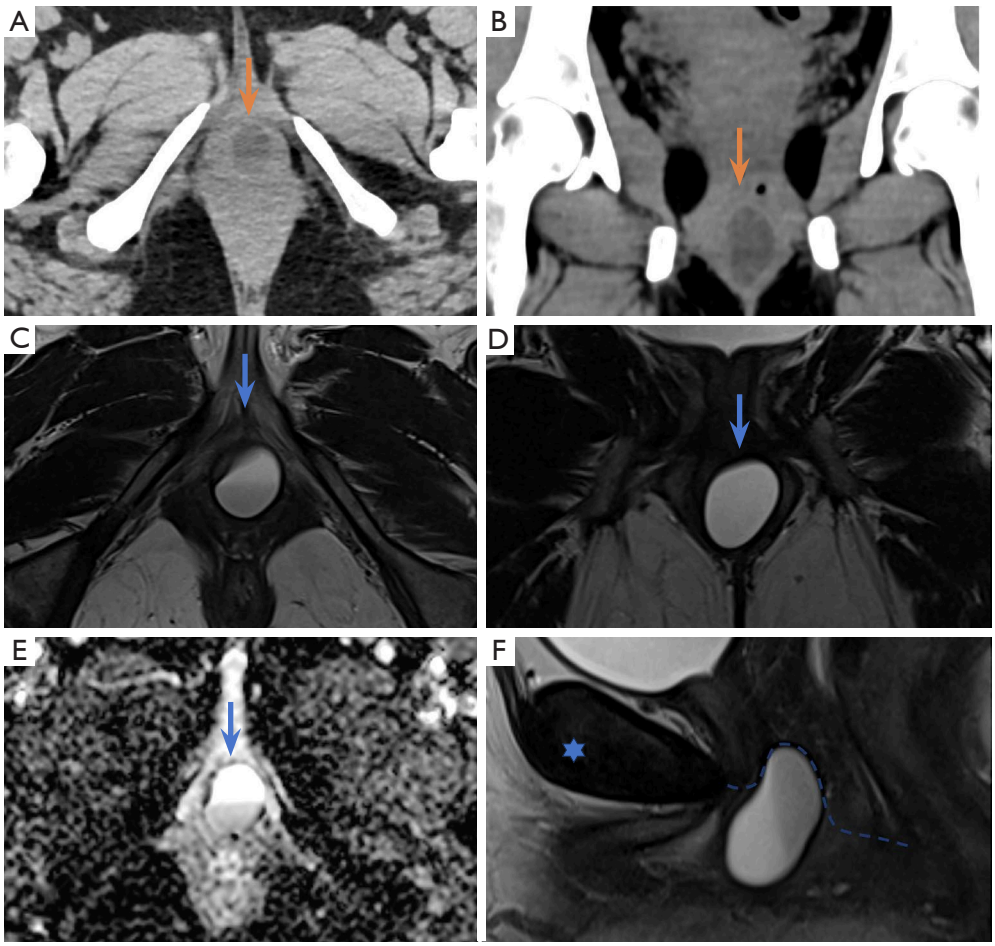

Figure 8 Non-contrast CT (pyelo-CT) and MRI correlation of a Skene's gland cyst. (A,B) CT: oval, hypodense paraurethral lesion (20 mm × 31 mm) lateralized to the left (orange arrows). (C-F) MRI: a well-defined cyst with no urethral communication and normal urethral wall signal (blue arrows). Sagittal T2 image (F) shows displacement of the perineal membrane (blue dotted line) and relation to the pubic bone (asterisk). CT, computed tomography; MRI, magnetic resonance imaging.

lesions in cases of anatomical proximity to those areas.

On MRI, epidermal inclusion cysts (*Figure 11*) appear as well-defined, rounded lesions located in the dermal or subdermal plane, with high signal intensity on T2 sequences. They may show subtle peripheral enhancement and diffusion restriction, depending on their content (4,5).

Neoplastic paraurethral-paravaginal lesions

Neoplasia of the proximal third of the urethra: leiomyoma

Leiomyoma is a benign neoplasia of smooth muscle. It is the most frequent benign etiology of the proximal third of the paraurethra and the most frequent gynecological pelvic neoplasia in childbearing age, with pure urethral involvement being its least common form of presentation (28,29). The mean age of presentation is 40 years. Symptoms are related to urethral obstruction and generally manifest as recurrent urinary tract infections, pelvic pain and dyspareunia. Surgical management is indicated in symptomatic patients (1,2,5,28,29).

In MRI, leiomyomas (*Figure 12*) appear as tumors or nodules of variable size, with lesions ranging from a few millimeters to large lesions. They are well-defined and their signal characteristics are like those of other leiomyomas in the rest of the body, with intermediate/low signal in T2-

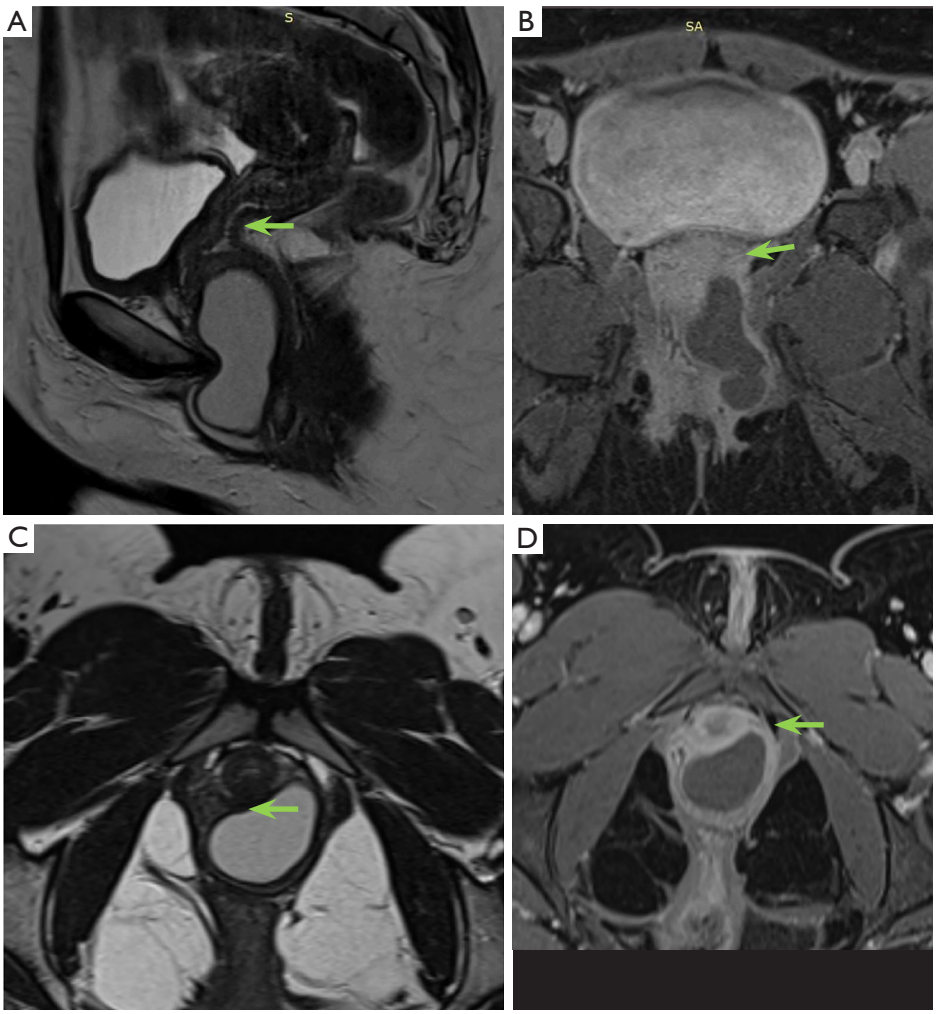

Figure 9 Gartner's duct cyst on contrast-enhanced pelvic MRI. Multilobulated cystic lesion (green arrows) in the anterosuperior vaginal wall, hyperintense on T2 (A,C), hypointense on fat-saturated T1 (B,D), with subtle wall enhancement. MRI, magnetic resonance imaging.

weighted sequences, isointense in T1 sequences, without restriction to diffusion sequence studies, and with variable impregnation in contrast-enhanced studies.

Neoplasia of the middle and distal third of the urethra: squamous cell carcinoma

At this level, the urethra is lined by squamous epithelium, for this reason the most frequent malignant neoplasia is squamous cell carcinoma. However, this neoplasia is globally rare with an incidence of 1.5 per million inhabitants in the female population (6,17,19,21,30). It generally manifests with a palpable mass, hematuria, dysuria and perineal pain. Some series have reported risk factors including urethral stricture, history of sexually transmitted infections and exposure to human papillomavirus (18). Dissemination is usually lymphatic towards superficial and deep inguinal chains, while hematogenous dissemination is rare. The optimal treatment is not fully defined; multimodal schemes with surgery, chemotherapy and radiotherapy have been proposed, with variable results (20).

On MRI, squamous cell carcinoma (*Figure 13*) appears as a solid urethral lesion with intermediate T2 and low T1 signal, diffusion restriction with low ADC values, and contrast enhancement. It is typically located below the perineal membrane in the mid-to-distal urethra and may protrude through the meatus. MRI also allows assessment

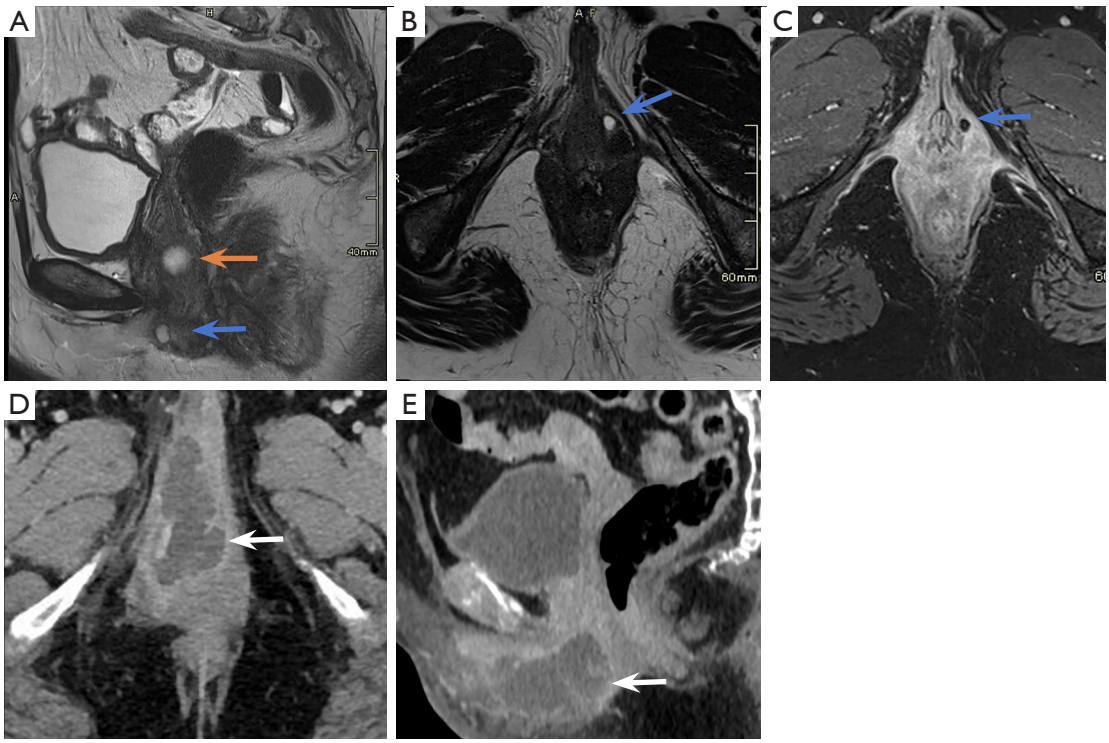

Figure 10 Bartholin's gland cyst with and without superinfection. (A-C) MRI: uncomplicated cyst (blue arrows), hyperintense on T2, located below the perineal membrane. No enhancement is seen on VSD (C). A urethral diverticulum is also visible (orange arrow). (D,E) CT: superinfected Bartholin's cyst with multilobulated wall, septations, and peripheral enhancement (white arrows). CT, computed tomography; MRI, magnetic resonance imaging; VSD, vaginal saline distension.

of muscular and transmural invasion (2,3,5).

Neoplasia of the proximal third of the urethra: urothelial carcinoma

Isolated manifestation in the urethra is rare, it is usually found in the context of a bladder neoplasia with extension to the urethra. When confined to the urethra, this subtype is less common than squamous cell carcinoma, although it shares similar clinical features and risk factors. From the clinical and imaging point of view, they can be indistinguishable (19,21,30). Both urothelial and squamous carcinomas are staged according to the standards provided by the American Joint Committee on Cancer (AJCC), which broadly considers local dissemination (bladder neck, vagina and vulva), lymph node dissemination and hematogenous dissemination 19).

MRI is the study of choice to determine the local extent of the disease. Carcinomas usually have hypointensity of signal in both T1 and T2 sequence (*Figure 14*), enhancement with IVC is variable, but there is a tendency to present discrete enhancements of hypovascular type, with significant restriction in diffusion sequence (3,4,19,21,30).

Vulvar-vaginal melanoma

These melanoma subtypes have a similar prognosis and staging factors as other cutaneous melanomas. The highest incidence is between 60 and 70 years of age. They are rare neoplasms; in the vulva and vagina, they account for less than 5% of all perineal malignancies and less than 2% of all melanomas. They are asymptomatic until very advanced stages. The prognosis tends to be poor, with a 5-year survival rate of 25% for vulvar melanoma and 15% for vaginal melanoma (13,31).

MRI is the study of choice for evaluating local involvement and presurgical planning. Melanomas may appear as vulvar or vaginal masses with an infiltrative

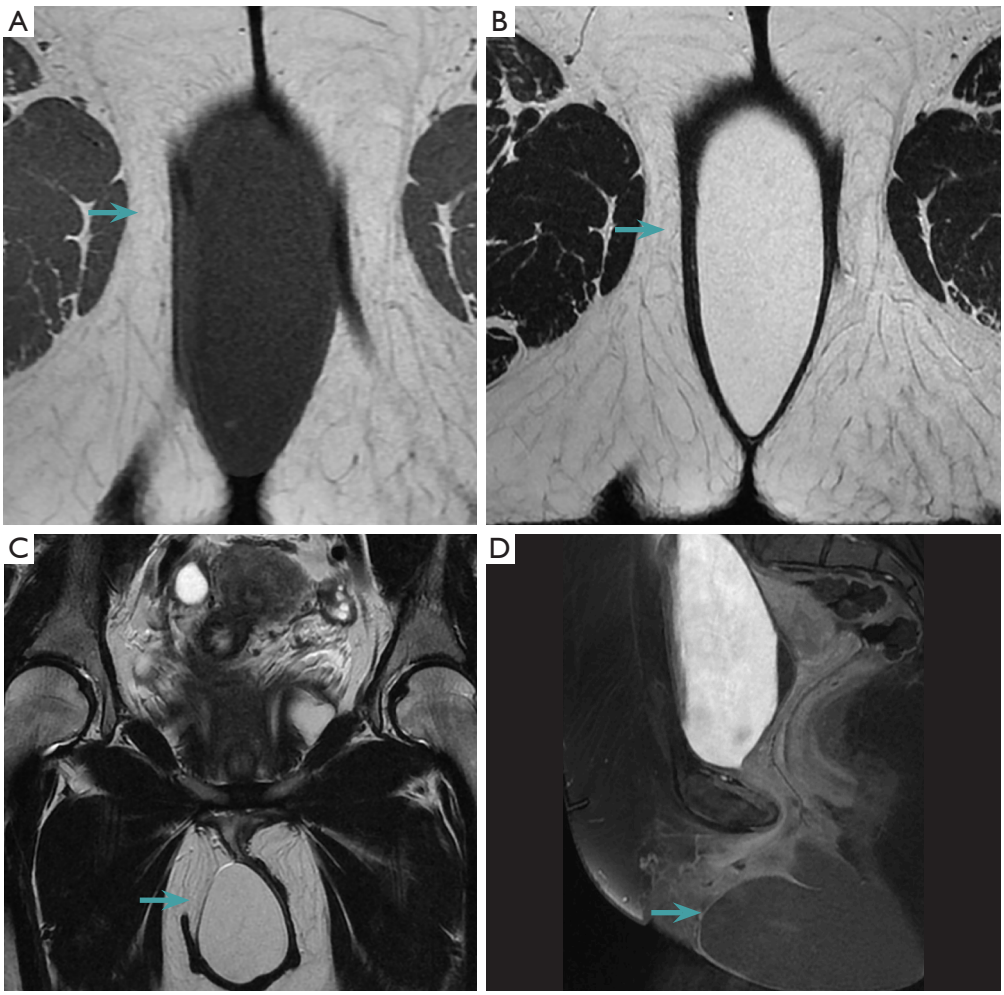

Figure 11 Epidermal inclusion cyst. VSD-enhanced pelvic MRI shows a large vulvar cyst (green arrows) below the perineal membrane, hypointense on T1 (A,D), hyperintense on T2 (B,C), with no significant enhancement on VSD (D). MRI, magnetic resonance imaging; VSD, vaginal saline distension.

pattern and high signal on both T1 and T2 sequences (*Figure 15*), due to melanin content—a key diagnostic clue. They may show early, slightly heterogeneous enhancement that tends to homogenize in delayed phases, along with diffuse and homogeneous diffusion restriction. Amelanotic melanomas, more common in this location, may appear hypointense on T1 (19,21,30).

Paraurethral-paravaginal lesions, miscellaneous

Paraurethral caruncle

This is the most common paraurethral lesion in postmenopausal women, representing more than 90% of paraurethral lesions in this population. Most patients are asymptomatic, but in isolated cases, they can cause pain and dysuria, especially when there is thrombosis or ischemia. From a pathological point of view, it corresponds to a squamous hyperplasia of the mucosa, with prolapse in the external urethral meatus, almost always based on the ventral aspect of the meatus, triggered by the hypoestrogenic environment. Initial treatment includes topical estrogens, and in the absence of response, surgical excision is suggested to rule out malignancy, which is found in less than 3% of lesions (32).

In MRI, caruncles (*Figure 16*) are visualized as a nodular thickening of soft tissues in the external urethral meatus,

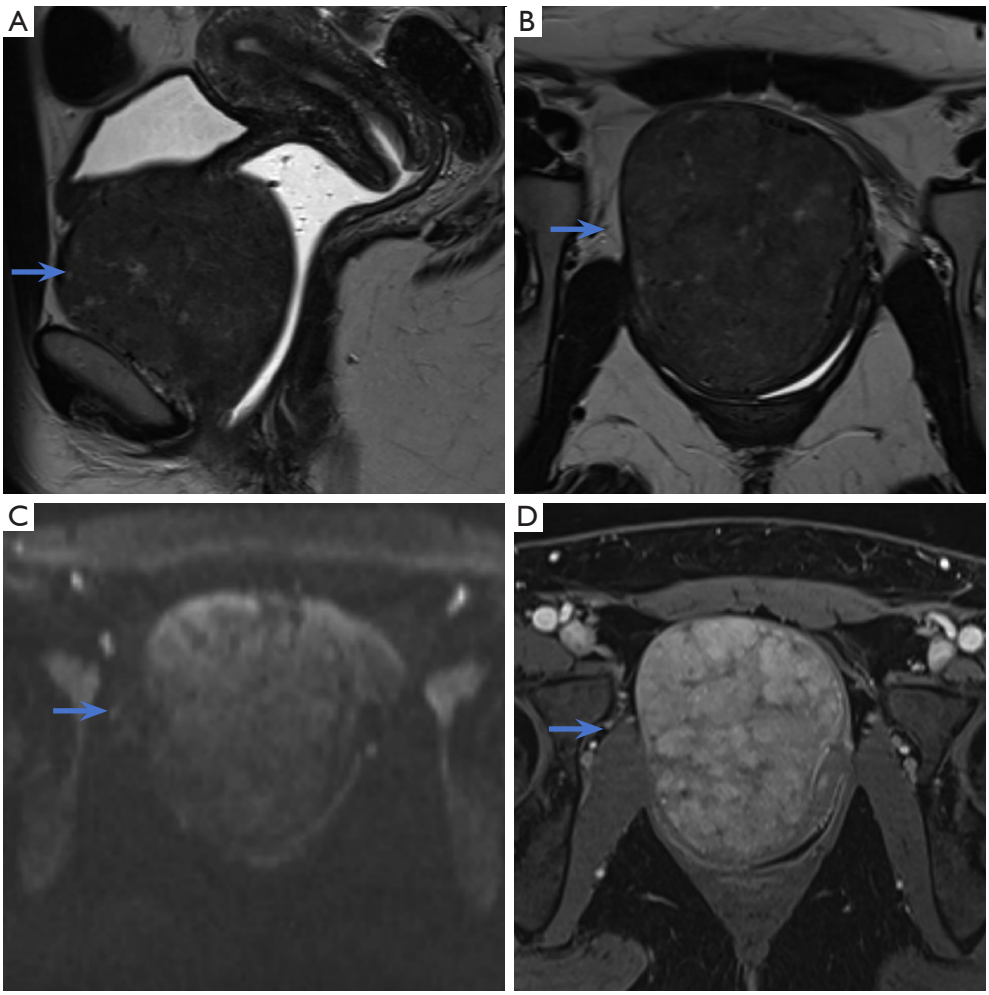

Figure 12 Urethral leiomyoma. VSD-enhanced pelvic MRI shows a well-defined mass (blue arrows) in the proximal right urethra, displacing the urethra leftward and vagina posteriorly. Slightly hypointense on T2 (A,B), with restricted diffusion (C) and heterogeneous contrast enhancement (D). MRI, magnetic resonance imaging; VSD, vaginal saline distension.

5 to 20 mm in length, which usually displace the urethra anteriorly. Rarely, malignant elements can be characterized by MRI when they are suspected from a clinical point of view, showing a signal like the mucosa in all sequences, and may have greater impregnation in the contrast study in case of local inflammation (5,32).

Conclusions

Paraurethral and paravaginal lesions in women are rare diagnoses but present distinctive features that are effectively assessed using MRI. Recognizing and differentiating these lesions is important to ensure an accurate diagnosis and guide optimal patient care. MRI is a fundamental imaging modality

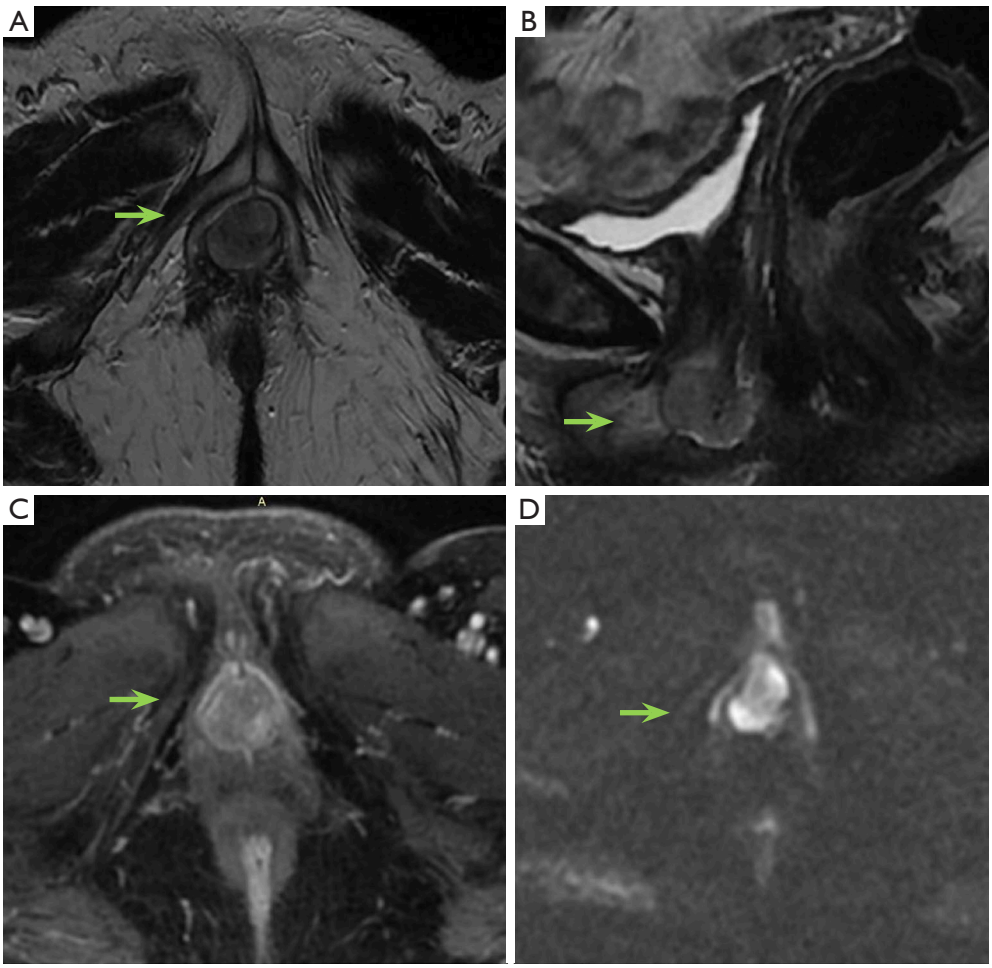

Figure 13 Squamous cell carcinoma of the distal urethra. MRI with VSD reveals a nodular lesion (green arrows) protruding toward the external urethral meatus. (A,B) Intermediate T2 signal; (C,D) marked diffusion restriction. Histopathology confirmed squamous cell carcinoma. MRI, magnetic resonance imaging; VSD, vaginal saline distension.

that provides comprehensive information on the most prevalent pathologies, as well as a spectrum of relevant differential diagnoses, allowing to distinguish between benign and malignant conditions. Its value is particularly evident in complex cases or when concurrent pathologies are suspected.

To ensure the best patient outcomes, both radiologists and urologists must be familiar with the topographic distribution of these lesions and the clinical implications of a correct diagnosis. This multidisciplinary knowledge facilitates more accurate assessments and contributes to improved, personalized treatment strategies.

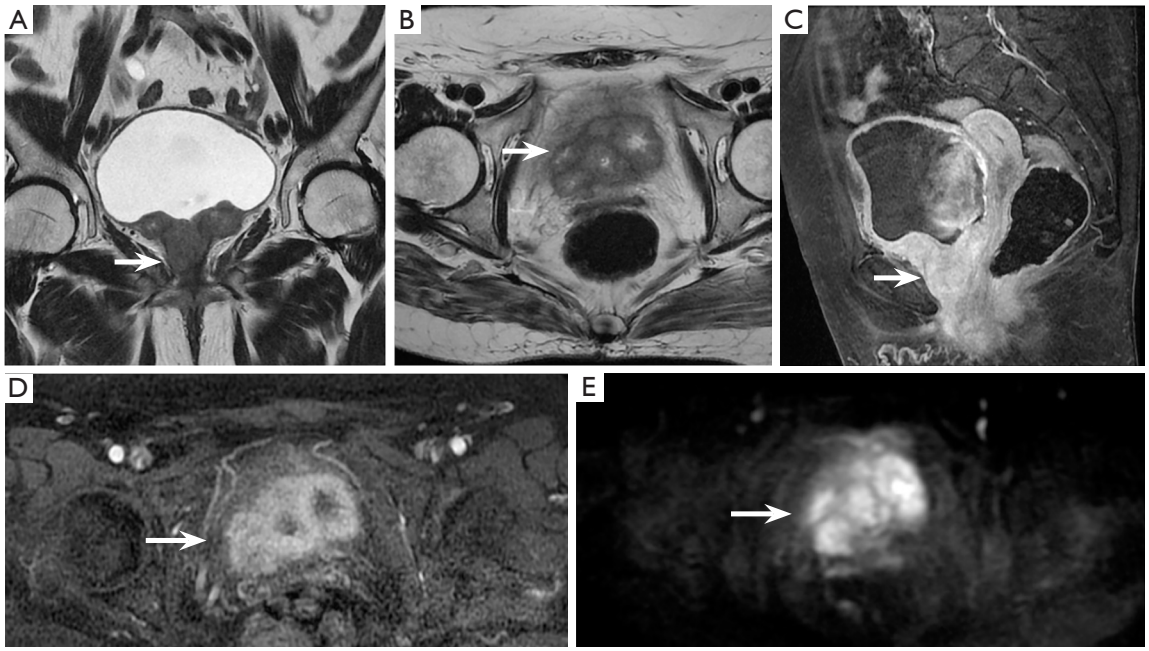

Figure 14 Urothelial carcinoma. VSD-enhanced pelvic MRI shows a neoplastic lesion (white arrows) involving the proximal urethra and bladder neck. T2 images show intermediate signal and necrosis (A,B), with contrast enhancement (C,D) and restricted diffusion (E). Histology confirmed urothelial carcinoma. MRI, magnetic resonance imaging; VSD, vaginal saline distension.

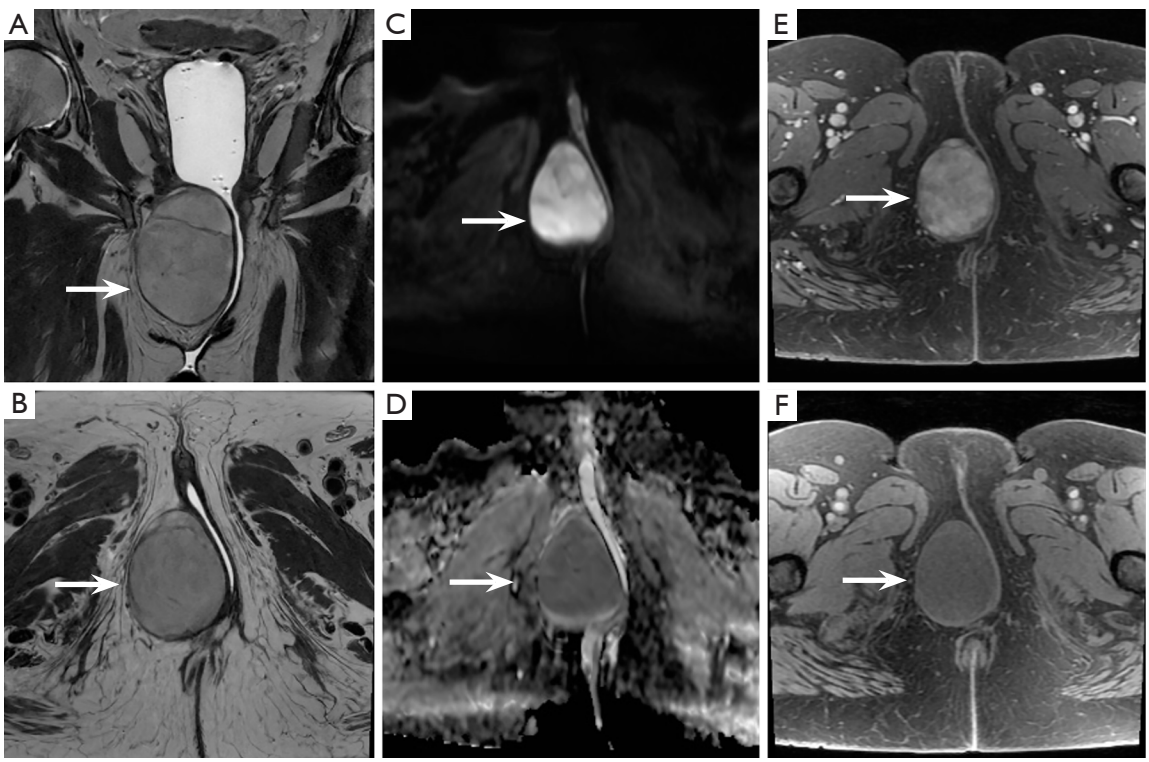

Figure 15 Subcutaneous vulvar neoplastic lesion. MRI with IVC and intravaginal gel shows a right subcutaneous lesion (white arrows) abutting the vaginal wall without invasion. (A,B) Intermediate T2 signal; (C,D) restricted diffusion; (E,F) heterogeneous enhancement. IVC, intravenous contrast; MRI, magnetic resonance imaging.

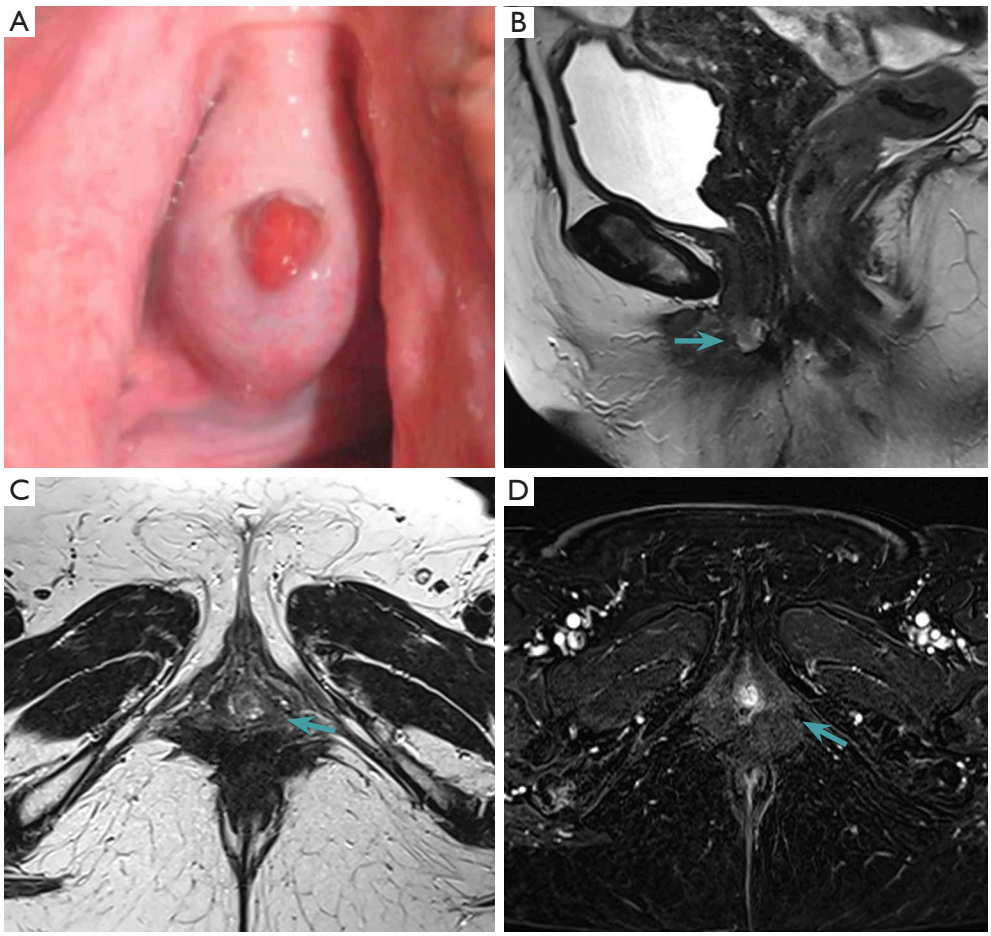

Figure 16 Paraurethral caruncle. Preoperative photo (A) and MRI with VSD show a nodular lesion (green arrows) below the perineal membrane, with mild hyperintensity on T2 (B,C) and peripheral enhancement on post-contrast images (D). MRI, magnetic resonance imaging; VSD, vaginal saline distension.

Acknowledgments

None.

Footnote

Peer Review File: Available at https://tau.amegroups.com/article/view/10.21037/tau-2024-726/prf

Funding: This work was funded by Clínica Alemana de Santiago and its Academic Department.

Conflicts of Interest: All authors have completed the ICMJE uniform disclosure form (available at https://tau.amegroups.com/article/view/10.21037/tau-2024-726/coif). The authors have no conflicts of interest to declare.

Ethical Statement: The authors are accountable for all aspects of the work in ensuring that questions related to the accuracy or integrity of any part of the work are appropriately investigated and resolved. This study was conducted in accordance with the Declaration of Helsinki and its subsequent amendments. All patients provided written informed consent for the use of their clinical information and anonymized imaging for scientific and educational publication purposes.

References

1. Tunn R, Petri E. Introital and transvaginal ultrasound as the main tool in the assessment of urogenital and pelvic floor dysfunction: an imaging panel and practical approach. Ultrasound Obstet Gynecol 2003;22:205-13.
2. Surabhi VR, Menias CO, George V, et al. Magnetic resonance imaging of female urethral and periurethral disorders. Radiol Clin North Am 2013;51:941-53.
3. Chaudhari VV, Patel MK, Douek M, et al. MR imaging and US of female urethral and periurethral disease. Radiographics 2010;30:1857-74.
4. Itani M, Kielar A, Menias CO, et al. MRI of female urethra and periurethral pathologies. Int Urogynecol J 2016;27:195-204.
5. Hosseinzadeh K, Heller MT, Houshmand G. Imaging of the female perineum in adults. Radiographics 2012;32:E129-68.
6. Kaufman ME, Miller DT, Ullah A, et al. Skene's Gland Adenocarcinoma: Borrowing From Prostate Cancer Experience for the Evaluation and Management of a Rare Malignancy. Urology 2021;151:182-7.
7. Chou CP, Levenson RB, Elsayes KM, et al. Imaging of female urethral diverticulum: an update. Radiographics 2008;28:1917-30.
8. Busto Martín L, Barguti I, Andraca AZ, et al. Cyst of the skene's gland: report of four cases and bibliographic review. Arch Esp Urol 2010;63:238-42.
9. Bats AS, Metzger U, Le Frere-Belda MA, et al. Malignant transformation of Gartner cyst. Int J Gynecol Cancer 2009;19:1655-7.
10. Wechter ME, Wu JM, Marzano D, et al. Management of Bartholin duct cysts and abscesses: a systematic review. Obstet Gynecol Surv 2009;64:395-404.
11. Del Gaizo A, Silva AC, Lam-Himlin DM, et al. Magnetic resonance imaging of solid urethral and peri-urethral lesions. Insights Imaging 2013;4:461-9.
12. O'Connor E, Iatropoulou D, Hashimoto S, et al. Urethral diverticulum carcinoma in females-a case series and review of the English and Japanese literature. Transl Androl Urol 2018;7:703-29.
13. Boer FL, Ten Eikelder MLG, Kapiteijn EH, et al. Vulvar malignant melanoma: Pathogenesis, clinical behaviour and management: Review of the literature. Cancer Treat Rev 2019;73:91-103.
14. Neitlich JD Foster HE Jr, Glickman MG, et al. Detection of urethral diverticula in women: comparison of a high resolution fast spin echo technique with double balloon urethrography. J Urol 1998;159:408-10.
15. Reeves FA, Inman RD, Chapple CR. Management of symptomatic urethral diverticula in women: a single-centre experience. Eur Urol 2014;66:164-72.
16. Saidman JM, Aineseder M, Garratt J, et al. Imaging the Female Urethra: US and MRI in Cystic and Solid Pathologic Conditions. Radiographics 2025;45:e240064.
17. Li XH, Zhang YT. Skene gland adenocarcinoma of the urethra: A systematic review. Asian J Surg 2024;47:1587-8.
18. Tubay M, Hostetler V, Tujo C, et al. What is that cyst? Common cystic lesions of the female lower genitourinary tract. RadioGraphics 2014;34:427-8.
19. Swartz MA, Porter MP, Lin DW, et al. Incidence of primary urethral carcinoma in the United States. Urology 2006;68:1164-8.
20. Blander DS, Rovner ES, Schnall MD, et al. Endoluminal magnetic resonance imaging in the evaluation of urethral diverticula in women. Urology 2001;57:660-5.
21. Derksen JW, Visser O, de la Rivière GB, et al. Primary urethral carcinoma in females: an epidemiologic study on demographical factors, histological types, tumour stage and survival. World J Urol 2013;31:147-53.
22. Dwyer PL, Rosamilia A. Congenital urogenital anomalies that are associated with the persistence of Gartner's duct: a review. Am J Obstet Gynecol 2006;195:354-9.
23. Heller DS. Vaginal cysts: a pathology review. J Low Genit Tract Dis 2012;16:140-4.
24. Choe J, Wortman JR, Sodickson AD, et al. Imaging of Acute Conditions of the Perineum. Radiographics 2018;38:1111-30.
25. Prasad SR, Menias CO, Narra VR, et al. Cross-sectional imaging of the female urethra: technique and results. Radiographics 2005;25:749-61.
26. Hoogendam JP, Smink M. Gartner's Duct Cyst. N Engl J Med 2017;376:e27.
27. Apostolis CA, Von Bargen EC, DiSciullo AJ. Atypical presentation of a vaginal epithelial inclusion cyst. J Minim Invasive Gynecol 2012;19:654-7.
28. Contreras-Albavera EO, Delgado-Gutiérrez GRI, Mandujano-Álvarez GJ, et al. Leiomioma en uretra femenina. Reporte de un caso. Ginecol Obstet Mex 2017;85:778-82.
29. Slaoui A, Lasri A, Karmouni T, et al. Leiomyoma: a case

report of a rare benign tumor of the female urethra. Pan Afr Med J 2015;22:111.
30. Vikram R, Sandler CM, Ng CS. Imaging and staging of transitional cell carcinoma: part 1, lower urinary tract. AJR Am J Roentgenol 2009;192:1481-7.
31. Mert I, Semaan A, Winer I, et al. Vulvar/vaginal melanoma: an updated surveillance epidemiology and end results database review, comparison with cutaneous melanoma and significance of racial disparities. Int J Gynecol Cancer 2013;23:1118-25.
32. Verma V, Pradhan A. Management of urethral caruncle - A systematic review of the current literature. Eur J Obstet Gynecol Reprod Biol 2020;248:5-8.

Cite this article as: Labra A, Cocio R, Saavedra Á, Schiappacasse G, Blaskovic F. Magnetic resonance imaging of paraurethral and paravaginal lesion: relevant diagnoses, key findings and surgical correlation. Transl Androl Urol 2025;14(5):1484-1502. doi: 10.21037/tau-2024-726